US-LHC IR MAGNET ERROR ANALYSIS AND COMPENSATION

J. Wei, V. Ptitsin, F. Pilat, S. Tepikian, Brookhaven National Laboratory, Upton, NY 11973, U.S.A.
N. Gelfand, W. Wan, J. Holt, Fermi National Accelerator Laboratory, Batavia, IL 60510, U.S.A.

Abstract

This paper studies the impact of the insertion-region (IR) magnet field errors on LHC collision performance. Compensation schemes including magnet orientation optimization, body-end compensation, tuning shims, and local nonlinear correction are shown to be highly effective.

1 INTRODUCTION

Performance of the Large Hadron Collider (LHC) at collision depends on achieving the highest possible magnet field quality and alignment accuracy in the IR triplet quadrupoles (MQX) and dipoles (D1) during low-β^* operation when beams cross at a design crossing angle Φ. These superconducting magnets[1] will be mainly built in the USA (BNL and FNAL, Fig. 1) and in Japan, and assembled in cryostats in the USA. Table 1 lists the major beam and machine parameters. A schematic layout is given in Fig. 2. In Section 2, we evaluate the LHC dynamic aperture (DA) under nominal LHC collision conditions[2] based on the expected construction and measurement errors of these magnets. In Section 3, we summarize the proposed compensation schemes.
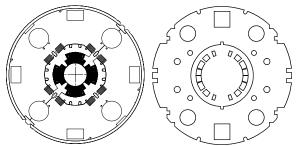

Figure 1: Magnet body cross section of FNAL-built MQX (left) and BNL-built D1 (right).

Table 1: LHC IR Parameters at proton collision (7 TeV).

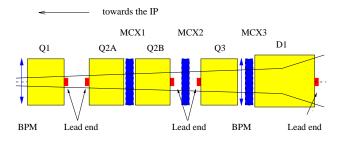|	
Betatron tunes (H/V)	63.31/59.32
Synchrotron tune	0.00212
Chromaticity (H/V)	2/2
β^*, IP1, 5, 2, 8 (H/V) [m]	0.5/0.5, 0.5/0.5, 15/10, 13/15
$\Phi/2$, IP1, 5, 2, 8 (H/V) [μr]	0/150, 150/0, 0/-150, 0/-150
Parallel sept., IP2, 8 [mm]	(H) 0.75, 0.75
Parasitic sept., IP1, 5, 2, 8 [σ_{xy}]	> 7.3, 7.3, 17, 18
Quad gradient, $|G_0|$ [T/m]	200
Coil i.d., MQX/D1,2 [mm]	70/80
Length, Q1,3/Q2A,B/D1,2 [m]	6.3/5.5/9.45
Max. β [m]	4705
rms emittance, ϵ_N [m·r]	3.75×10^{-6}
rms momentum dev., σ_p	1.1×10^{-4}
Max. rms beam size, σ_{xy} [mm]	1.5
Max. orbit offset (H/V) [mm]	$\pm 7.3/\pm 7.3$

Figure 2: Schematic layout of the LHC inner triplet region.

Since the beam size varies significantly along the length of the IR magnets, systematic transverse fringe-field[3] components are treated separately. The body harmonics are expressed in "units" of 10^{-4} of the magnet integral strength at the reference radius of 17 mm.[4] The lead-end (LE) and return-end (RE) harmonics are expressed in an integrated form in unit-meters. Tables 2 and 3 list expected[5, 6] values of the mean ($\langle b_n \rangle$, $\langle a_n \rangle$), uncertainty in mean ($d(b_n)$, $d(a_n)$), and standard deviation ($\sigma(b_n)$, $\sigma(a_n)$) of the body, lead-end, and return-end harmonics of the FNAL-built[7] quadrupoles MQX and BNL-built dipoles D1.

2 TRACKING RESULTS AT COLLISION

The impact of magnetic errors is assessed by the maximum tune spread among particles with amplitudes of up to 6 times the transverse rms beam size ($6\sigma_{xy}$), and by the DA from 6D tracking of either 10^5 or 10^3 turns of particles of initially up to 2.5 times rms momentum deviation ($2.5\sigma_p$) at 5 horizontal-to-vertical emittance ratios ϵ_x/ϵ_y. End effects are modelled as lumped kicks.[3] Table 4 shows the

Table 2: Expected field errors of FNAL-built IR quadrupole (MQX) at collision (version 1.1, $R_{ref} = 17$ mm).

n	Normal			Skew		
	$\langle b_n \rangle$	$d(b_n)$	$\sigma(b_n)$	$\langle a_n \rangle$	$d(a_n)$	$\sigma(a_n)$
Body	[unit]					
3	0.0	0.34	0.85	0.0	0.34	0.85
4	0.0	0.26	0.87	0.0	0.26	0.87
5	0.0	0.20	0.34	0.0	0.20	0.34
6	0.0	0.17	0.25	0.0	0.17	0.25
7	0.0	0.14	0.11	0.0	0.14	0.11
8	0.0	0.10	0.07	0.0	0.10	0.07
9	0.0	0.08	0.07	0.0	0.08	0.07
10	0.0	0.06	0.03	0.0	0.06	0.03
LE	[unit·m]		(Length=0.41 m)			
2	0.0	0.0	0.0	16.0	0.0	0.0
6	2.3	0.0	0.0	0.07	0.0	0.0
10	-0.09	0.0	0.0	-0.03	0.0	0.0
RE	[unit·m]		(Length=0.33 m)			
6	0.39	0.0	0.0	0.0	0.0	0.0
10	-0.07	0.0	0.0	0.0	0.0	0.0

Table 3: Expected field errors of BNL-built IR dipole (D1 at IP2, 8) at collision (version 1.0, $R_{ref} = 17$ mm).

n	Normal			Skew		
	$\langle b_n \rangle$	$d(b_n)$	$\sigma(b_n)$	$\langle a_n \rangle$	$d(a_n)$	$\sigma(a_n)$
Body	[unit]					
2	0.07	0.54	0.19	0.43	2.4	1.1
3	-1.5	1.6	0.84	-0.12	0.27	0.10
4	0.00	0.08	0.03	0.01	0.34	0.13
5	0.11	0.17	0.09	-0.01	0.04	0.01
7	0.11	0.02	0.01	-0.00	0.01	0.00
9	0.00	0.01	0.00	-0.00	0.00	0.00
LE	[unit·m]		(Length=0.73 m)			
2	-0.32	1.5	0.67	-0.97	2.9	1.2
3	10.3	1.4	0.51	-4.6	0.47	0.18
5	-0.09	0.15	0.05	0.48	0.06	0.03
RE	[unit·m]		(Length=0.73 m)			
2	0.15	1.2	0.45	0.62	3.1	1.3
3	2.8	1.2	0.54	0.13	0.48	0.16

Table 4: Effects of MQX and D1, D2 errors in terms of 10^3-turn 6D DA and 4D $6\sigma_{xy}$ maximum tune spread.

Case	DA (σ_{xy})	Min. DA	$\Delta\nu_{max}$ (10^{-3})
Full error (incl. a_2)	9.6±2.8	$6\sigma_{xy}$	coupled
Full error, $\Phi = 0$	12.7±1.8	$9\sigma_{xy}$	coupled[8]
Full error excl. a_2	10.7±1.7	$8\sigma_{xy}$	1.9±1.1
Systematic only	11.2±1.0	$10\sigma_{xy}$	2.6
Random only	13.6±1.7[a]	$9\sigma_{xy}$	1.1±0.5
LE and RE only	16.4±1.0[a]	$13\sigma_{xy}$	0.7
$n = 3, 4$ only	21.7±5.8[a,b]	$12\sigma_{xy}$	1.1±0.6
IR dipoles only	physical ap.[a]		0.2±0.01

a) Here, MQX physical aperture of 60 mm corresponds to 15.8±1.3σ_{xy}. Step size is $1\sigma_{xy}$ for 10^3; $0.5\sigma_{xy}$ for 10^5 DA.
b) The working point is near 3rd-order integer.

effects of magnetic errors expressed in terms of the mean and standard deviation (SD) of $6\sigma_{xy}$ maximum tune spread obtained with 4D tracking, and 10^3-turn DA. 10 sets of random errors are studied, each Gaussian distributed and truncated at 3 times rms. Systematic errors are assumed to contain their full uncertainty $d(b_n, a_n)$ with the signs correctly determined in accordance to the magnet orientation. Each quadrupole is modeled with 8 thin body pieces and 2 end (LE, RE) pieces. Obviously, the effect of IR dipoles is negligible due to the high β^* at IP2 and 8. The effect of both MQX systematic and random errors are significant.
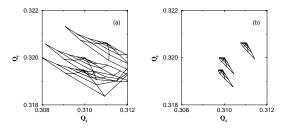

Figure 3: Effects of IR magnet errors at collision and the improvement with IR correctors (case 5 of Table 5).
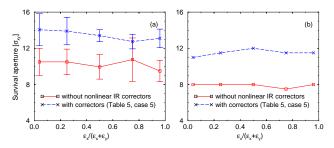

Figure 4: 10^5-turn (a) (mean±SD) and (b) minimum DA in 5 transverse directions showing the impact of IR magnet errors and the improvement with IR correctors.

Linear decoupling is essential.[2] Crossing angle ($\pm 150\mu$r) accounts for about $3\sigma_{xy}$ DA.[8] Comparing with 10^3-turn tracking, 10^5-turn tracking results in a further reduction in DA of less than $1\sigma_{xy}$. Fig. 3a shows typical $6\sigma_{xy}$ tune footprints for $\Delta p/p = 0, \pm 2.5\sigma_p$. Without compensation, the impact of MQX magnet errors is exceedingly large.

3   IR COMPENSATION SCHEMES

Error compensation is based on the minimization of action-angle kicks[9] produced by each multipole error b_n (or a_n) over a pair of inner triplets, i.e. minimizing the quantities

$$\int_L dl\beta_z^{n/2} B_0 b_n + (-)^n \int_R dl\beta_z^{n/2} B_0 b_n, \quad z = x, y \quad (1)$$

taking advantage of the negligible betatron phase advance within each triplet and D1, and approximate 180° phase advance between the triplets. The integral is over the entire left-side (L) or right-side (R) MQX triplet and D1. The quantity B_0 is the main field for dipoles and $G_0 R_{ref}$ for quadrupoles. Since two intersecting beams share these magnets, the compensation is designed for both beams in both the x and y directions without considering the closed-orbit deviation caused by the crossing angle.

3.1   Magnet Orientation Optimization

Fig. 5a shows typical tune spreads of about 0.002 produced by MQX end b_6 errors alone. This spread is reduced by more than a factor of 2 (Figs. 5b and c) by optimizing the orientation of MQX lead ends (see Fig. 2), cancelling b_6 effect between nearby focusing and defocusing quadrupoles.[9] The lead end of D1 is oriented away from the IP to minimize the effect of lead-end b_3.

3.2   Body-End Compensation

The impact of lead-end b_6 is further reduced (Fig. 5c) by adjusting the design value of body b_6 averaged across each
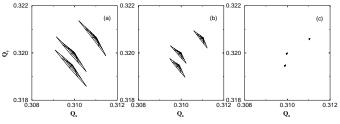

Figure 5: Effects of (a) MQX end b_6, (b) orientation optimization, and (c) body-end compensation.

Table 5: Comparison of IR correction efficiency using 10^3-turn 6D DA and 4D $6\sigma_{xy}$ maximum tune spread. Nonlinear corrections are activated in IP1 and 5 only. Also listed is the number of corrector layers per correction package.

Case	DA (σ_{xy})	Min. DA	$\Delta\nu_{max}$ (10^{-3})	layers
0	10.7±1.7	$8\sigma_{xy}$	1.9±1.1	1
1	10.7±1.3	$9\sigma_{xy}$	2.1±1.0	2
2	12.5±1.9	$9\sigma_{xy}$	1.9±1.5	2
3	13.3±1.6	$10\sigma_{xy}$	1.0±0.7	3
4	13.6±1.5	$11\sigma_{xy}$	0.5±0.3	4
5	14.1±1.5	$11\sigma_{xy}$	0.5±0.4	4

case 0: b_1, a_1, a_2
case 1: case 0 plus b_3, a_3, b_4
case 2: case 0 plus b_6, b_6, a_6
case 3: case 0 plus b_3, b_4, b_6, a_3, a_4, a_6
case 4: case 0 plus b_3, b_4, b_5, b_6, b_6, a_3, a_4, a_5, a_6
case 5: case 0 plus b_3, b_4, b_5, b_6, b_{10}, a_3, a_4, a_5, a_6

triplet according to the amplitude-weighted expression[9]

$$b_6(\mathrm{Body}) = -0.10\, B_6(\mathrm{LE}) - 0.23\, B_6(\mathrm{RE}) = -0.32\,[\mathrm{u}]$$

where B_6 is integrated b_6 in [u·m]. This choice of body b_6, same for all MQX magnets, is insensitive to lattice optics changes as long as β^* is small. Similarly, the desired body b_3 for the D1 dipole is (close to Table 3 value)

$$b_3(\mathrm{Body}) = -0.095\, B_3(\mathrm{LE}) - 0.116\, B_3(\mathrm{RE}) = -1.3\,[\mathrm{u}]$$

3.3 Magnetic Tuning Shims

After the construction and warm measurement of each FNAL-built MQX magnet, 8 tuning shims with adjustable iron thickness will be inserted into 8 slots (Fig. 1) to individually minimize body b_3/a_3 and b_4/a_4 errors. Table 2 includes the partial improvements expected.[10]

3.4 IR Correctors

Each triplet contains three corrector packages (MCX1, MCX2, MCX3), each consisting of as many as 4 layers of correction elements. For each multipole, two correction elements located symmetrically at opposite sides of the IP

Table 6: Proposed IR triplet correction strategy.

n	Normal (b_n)	Skew (a_n)	Corr. Strength [u·m][a] (b_n)	(a_n)
1	MCX1 (or 3)	MCX3 (or 1)	—[b]	—[b]
2	Trims	MCX2		—[b]
3	S, MCX1	S, MCX2	5.6±4.5	13.0±10.5
4	B, S, MCX3	S, MCX2	7.0±4.1	10.8±8.3
5	MCX1	MCX3	2.3±2.0	2.4±2.3
6	BE, MCX1	MCX2	5.4±1.9	3.5±3.1
8	B			
10	B, MCX3		0.5±0.3	

B: coil cross-section iteration
BE: cross-section iteration, magnet orientation, body-end compensation
S: using tuning shims
MCX1 – 3: using corrector MCX1, MCX2, or MCX3

a) normalized to 10^{-4} of MQX strength at 17 mm radius.
b) to be determined from magnet alignment errors.[2]

can be activated to minimize the kick (Eq. 1) in both the x and y directions (hence for both beams due to lattice symmetry). Assuming that magnetic errors are measured to a 10% rms accuracy, Table 5 compares various options of correction strategy. It shows that with 3 packages per triplet each consisting of 4 layers of multipole elements (cases 4 and 5), we achieve a tune spread of less than 10^{-3} (Fig.3b), an average DA larger than $12\sigma_{xy}$, and a minimum DA larger than $10\sigma_{xy}$ (Fig. 4 and Table 5). Table 6 lists the proposed correction strategy for each multipole candidate and the needed corrector strength (mean±SD, bipolar). The IR correctors are designed for reducing the impact of both D1 and MQX errors during low-β^* operations.

4 SOFTWARE BENCHMARKING

We obtained tune footprints and DA results using the TEAPOT program[11]. The agreement on analysis and tracking results (Table 7) between TEAPOT and MAD is satisfactory given the fact that MAD splits[12] each quadrupole into 4 pieces while TEAPOT splits into 8. Further benchmarking is under way using the Standard eXchange Format (SXF).[13]

Table 7: Comparison of TEAPOT and MAD tracking (10^3 and 5×10^4 turn, 4D, 5 transverse directions, $\Phi = 0$) with systematic errors in the MQX body only.

Emit. ratio $\epsilon_x/(\epsilon_x + \epsilon_y)$	MAD (10^3)	MAD (5×10^4)	TEAPOT (10^3)	TEAPOT (5×10^4)
0.04	17	17.0	17	16.5
0.25	17	17.0	18	17.0
0.50	17	16.0	18	17.0
0.75	16	15.0	16	14.0
0.96	16	16.0	16	14.5

5 REFERENCES

[1] D1 at IP1 and 5 are normal-conducting magnets whose error effects are not included in this study.

[2] The study uses LHC lattice version 5.1 excluding beam-beam effects and magnet misalignments. Except for the first two cases of Table 4, a_2 errors are not considered.

[3] J. Wei, R. Talman, Part. Accel., **55**, 339 (1996).

[4] European convention with $n = 1$ for dipole.

[5] LHC IR Design Mini-Workshop, FERMILAB 97/378 (1998).

[6] A. Jain, et al, these proceedings; RHIC/AP/147 (1998).

[7] Same errors are used for Japanese and FNAL built quads.

[8] V. Ptitsin, S. Tepikian, RHIC/AP/152 (1998).

[9] J. Wei, Part. Accel., **55**, 439 (1996); RHIC/AP/154 (1998).

[10] R. Bossert, et al, these proceedings.

[11] L. Schachinger, R. Talman, Part. Accel. **22**, 35 (1987).

[12] H. Grote, F.C. Iselin, CERN/SL/90-13 (1990).

[13] F. Pilat et al, RHIC/AP/155 (1998).